Desalination and Water Treatment
www.deswater.com
doi: 10.5004/dwt.2019.23185

137 (2019) 143–153
January

Adsorption of phenol onto alginate-adsorbent beads prepared from pine cone: equilibrium and factorial design methodology

Soumeya Bouchareb[a], Dalila Hank[a,b,*], Mohamed Abdel Salam[c], Kassia Ouddai[b], Amina Hellal[a]

[a]*Laboratoire des Sciences et Techniques de l'Environnement, Ecole Nationale Polytechnique, Alger, Algérie, Tel. +213 2152 53 01 / 03; Fax: +213 21 52 29 73, emails: dalila.hank@g.enp.edu.dz (D. Hank), bouchareb.soumeya@hotmail.com (S. Bouchareb), amina.hellal@g.enp.edu.dz (A. Hellal)*
[b]*Département Génie Rural, Ecole Nationale Supérieure Agronomique, Alger, Algérie, email: ouddai.kassia@gmail.com*
[c]*Department of Chemistry, Faculty of Science, King Abdulaziz University, Jeddah, KSA, email: masalam16@hotmail.com*

Received 20 March 2018; Accepted 23 September 2018

ABSTRACT

In this research study, the removal of phenol from aqueous solution was investigated in a batch system using a new adsorbent prepared from the pine cone. The raw pine cone was activated by chemical calcination and immobilized in alginate producing the alginate-powdered activated pine cone (alginate-PAPC) beads. The obtained biomaterial was characterized by infrared spectroscopy and scanning electron microscopy. The effects of solution pH, initial phenol concentration and alginate-PAPC beads mass on the adsorption process were studied. A factorial experimental design 2^3 was considered to investigate the effect of the three parameters on the equilibrium adsorption capacity. The equilibrium adsorption results can be successfully modeled by the Langmuir, Freundlich, and Temkin, isotherms. The maximal biosorption capacity was 146.39 mg of phenol/g alginate-PAPC beads and corresponds to 500 mg/L of initial phenol concentration, pH medium 2, and 1 g of alginate-PAPC beads mass.

Keywords: Adsorption; Alginate-PAPC beads; Full experimental design methodology; Phenol.

1. Introduction

Water pollution is one of the major environmental problems in the world due to rapid industrial development [1]. Phenol is often found in the wastewater from many industrial processes like resin manufacturing, oil refineries, pharmaceuticals, dyes, paper-processing plants, coal liquefaction, textiles, and plastic industries [2]. Therefore, it is generally recognized as toxic and is placed on the priority list of chemicals highly hazardous to the environment due to its corrosive nature [3]. Phenol removal from water and wastewater has been carried out by various technical processes including photocatalytic degradation [4], solvent extraction [5], microbial degradation [6], ion exchange [7], membrane process [8], forward osmosis process [9], and adsorption by solid adsorbents [10–13]. Removal of organic pollutants like phenol by adsorption is considered as one of the most effective processes for wastewater treatment without producing any harmful by-products with the possibility of regenerating pollutants as well as adsorbents. Activated carbon is considered as one of the most used solid adsorbent for the removal of phenol, and the phenolic compounds from polluted water [14–17]. Nowadays, one of the great challenges in the adsorption technologies is the exploring of new potential and low-cost adsorbents which could be used successfully for the removal of phenol from polluted water. Conventional separation methods such as electrochemical oxidation, photo-oxidation, ozonation, UV/H_2O_2, Fenton reaction, membrane processes, and enzymatic treatments,

* Corresponding author.

have been effective for organic pollutants removal from aqueous environments. But their high costs, slow turnaround time and consumption of chemicals, have restricted their applicability. Of the removal methods, adsorption is one that is gaining increasing attention due to its potential efficiency, low energy consumption, high selectivity at molecular level, easy operation, and ability to separate various chemical compounds [18].

Agricultural wastes are natural materials available in large quantities at no or low cost. Renewable products from industrial or agricultural operations have been recognized as new adsorbents for different water pollutants. For example, banana peels were used for the removal of radioactive minerals [19], internal almond shell, sheep manure waste and sawdust were used for the removal of methylene blue [20], sugarcane bagasse, rice husk, and castor leaves were used for the removal of heavy metals [21]. The antibiotic tetracycline was removed by rice husk ash [22], and nitrate ions were removed by amine-grafted ground coconut copra and corn cob particles [23]. Although the application of low-cost agriculture waste for the removal of phenol as an organic pollutant from water is scarce in the literature [1,24–26], more research work is required to explore new efficient low-cost adsorbents based on agriculture waste.

In the present research, we studied the performance of a low-cost adsorbent prepared from pine cone, Alginate-PAPC beads, for the removal of phenol from aqueous solution. The powdered pine cone was pretreated to increase its adsorption properties and immobilized in calcium alginate beads to overcome problems due to its small particle size [27] and to facilitate the separation of the biosorbent from the aqueous solution [2].

The effects of various adsorption parameters such as adsorbent mass, pH solution, and initial phenol concentration on the adsorption using alginate-PAPC beads have been investigated. The effect of each parameter and their interaction on equilibrium adsorption capacity was determined using a full factorial experimental design methodology, and a statistical model of the process was developed.

Recently many statistical experimental design methods are used in the different chemical sector for optimization of process parameters. Experimental design is a group of mathematical and statistical techniques useful for analyzing the effects of several independent variables and their interactions [28,29]. It is used to identify the effective parameters and to optimize the response in a reduced number of experiments [30].

2. Material and methods

2.1. Preparation of powdered activated pine cone

Pinecone was collected from local forest plantations in Algiers, Algeria Fig. 1(a). It was washed with distilled water to remove impurities and then dried in an oven at 105°C for 24 h. Ten grams of the raw material was immersed in 100 mL of H_2SO_4 solution (40%) with a ratio of 1:10 proportion (weight/volume) and kept at 100°C for 1 h. The acid treated pine cone was repeatedly washed with deionized water and then dried at 105°C for 24 h. The obtained sample was calcined at 500°C for 2 h, crushed and sieved at a diameter ≤ 500 μm.

2.2. Preparation of alginate-PAPC beads

The desired amount of powdered activated pine cone (PAPC) was added to Sodium alginate (Fluka) solution 3% (w/v) [31]. The viscous solution was introduced into a burette and extruded through a needle of 5 mm diameter. The beads were pulled off on 100 mL of a 3 g/L $CaCl_2$ stirred solution and maintained for 2 h at 37°C to ensure more stable hydrogels. Then, the composite adsorbent was rinsed with distilled water and stored at 4°C Fig. 1(b).

2.3. Point zero charge determination

The organic functional groups on the biosorbent surface may acquire a negative or positive charge depending on the solution pH. The point of zero charge of the adsorbent was determined by the solid addition method. A 50 mL of 0.01 N NaCl solution was transferred into a series of 100 mL Erlenmeyer. The pH (pH_i) values of the solution were adjusted to 2, 4, 6, 8, 10 and 12 by adding either fixed strength of HCl (1N) or NaOH (1N). Then 0.1 g of activated pine cone was added to each flask which was securely capped immediately. The flask was then placed into a magnetic shaker for 24 h. The difference between the initial and final pH values ($\Delta pH = pH_f - pH_i$) was plotted against the pH_i. The point of intersection of the resulting curve at which $\Delta pH = 0$ gave the pH_{pzc}.

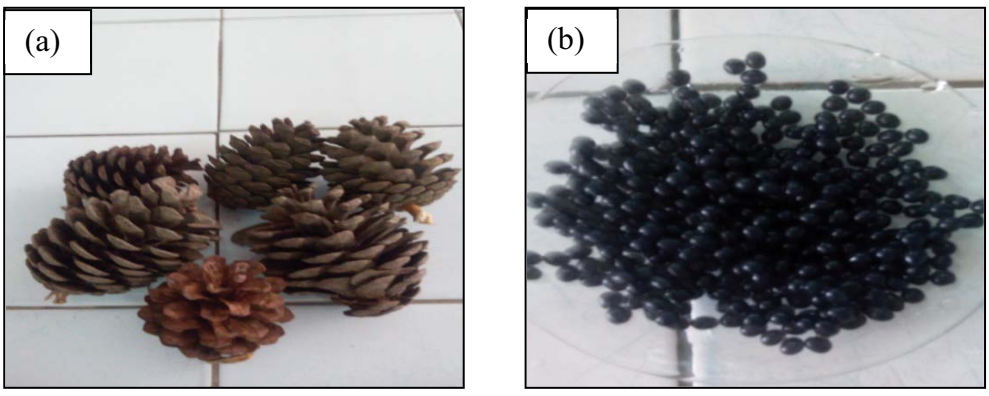

Fig. 1. Raw pine cones (a) alginate powdered activated pine cone beads (b).

2.4. Characterization of PAPC and alginate-PAPC beads

The FTIR spectra of PAPC was recorded on a Fourier transform infrared spectrometer (PERKIN-ELMER Model Spectrum One) to identify the characteristic of the functional groups in the range of 650–4,000 cm^{-1}.

A scanning electron microscope (SEM) (INSTRUMENT JSM-6360) was used to give information about the surface morphological structure of raw pine cone, powdered activated pinecone, alginate beads, and alginate-powdered activated pine cone beads.

2.5. Phenol analysis

The phenol concentration in the aqueous solution was determined by a spectrophotometric method based on the condensation of 4-aminoantipyrine with phenol in the presence of an oxidizing agent; potassium ferricyanide, to form a colored antipyrine dye under alkaline conditions [32]. The absorbance was measured at a 510 nm wavelength using a Shimadzu UV–VIS 1240 spectrophotometer.

2.6. Adsorption procedure

Adsorption experiments were carried out in a batch system with the Alginate-PAPC beads of 5 mm diameter and a ratio volume of alginate adsorbent and phenol solution 200:1,000. In the equilibrium isotherms study, 0.375 g of PAPC was added to the alginate for the beads preparation. Then the Alginate-PAPC beads obtained were added to 125 mL of phenol solution, and the mixture was shaken at 225 rpm under ambient temperature for 24 h to ensure equilibrium was reached. The range of initial phenol concentration was (20–500 mg/L). In pH studies, the solution pH was adjusted by the addition of HCl or NaOH (1N). The adsorption capacity expressed by the amount of phenol adsorbed at a time q_t (mg/g) and at equilibrium condition q_e (mg/g) was calculated according to the following equations:

$$q_t = \frac{(C_0 - C_t) \times V}{m} \quad (1)$$

$$q_e = \frac{(C_0 - C_e) \times V}{m} \quad (2)$$

where C_0 and C_e are the initial and the equilibrium adsorbate concentrations (mg/L), respectively. C_t is the adsorbate concentration at time (mg/L). V is the volume of solution (L), and m is the mass of adsorbent (g).

3. Results and discussions

3.1. Point zero charge

The pH_{zpc} of the solid surface is the pH values at which the amount of acidic and basic functional groups is equal. The organic functional groups on the biosorbent surface may acquire a negative or positive charge depending on the solution pH. For pH values greater than the p*K*a of acidic groups, the sites are mainly in dissociated from and acquire a negative charge, while at pH values lower than p*K*a of these groups will be associated with a proton to become positively charged [33]. Fig. 2 shows the plot of ΔpH versus pH_f. The pH_{zpc} of the biosorbent was found to be 6.1 indicating that the acidic groups are predominant on the surface of the adsorbent. The most suitable pH for the adsorption of the organic compounds is below the pH_{zpc}.

3.2. FTIR and SEM analyzes

Pinecone is composed of epidermal and sclerenchyma cells that contain cellulose, hemicellulose, lignin, rosin, and tannins in their cell walls with polar functional groups including alcohols, aldehydes, ketones, carboxyls, phenols and other groups [33–35]. Fig. 3 shows the FTIR spectra of the powdered activated pine cone which is composed of a mixture of functional groups [36]. A wide absorption band at 3,200–3,600 cm^{-1} with a maximum at about 3,425.44 cm^{-1} is due to O–H and N–H stretching groups [37,38].The bands at 2,926.26 cm^{-1} and 2,854.23 represent aliphatic C–H group [35]. The peaks at 1,453.52 cm^{-1}, 1,427.11 and 1,383.05 correspond to *N*-alkyl ted aromatic amines [33,38]. A peak at 1,275.57 cm^{-1} indicates C–N stretching with an amine or C–O vibration of carboxylic acid [35,38]. Bands at 1,159.32 and 1,111.86 cm^{-1} correspond to C–O stretching [38]. The peaks 158.89 cm^{-1} possibly assigned to the C–C stretching [39]. The peaks between 1,058.89, 876.46, and 559.32 cm^{-1} may be assigned to the C–C and C–N stretching, respectively [36,38].

The analysis of the pore structure of the powdered raw pine cone, the powdered activated pine cone (PAPC), the alginate beads, and the alginate PAPC beads by SEM is given in Figs. 4 and 5. The absence of the porous structure of the raw pine cone and the alginate beads can be seen in contrary to the PAPC and the alginate-PAPC beads which possess a good porous structure. For further study, the alginate-PAPC was used as an adsorbent for the phenol elimination from the water.

3.3. Effect of adsorbent mass

The adsorption of phenol onto alginate-PAPC beads was studied by varying the adsorbent dose (1–5 mg/500 mL) for 100 mg/L of phenol concentration. The adsorption capacity increased from 17.19 to 36.84 mg/g with the PAPC dose in alginate beads increasing from 1 to 5 g/L at equilibrium time as can be seen in Fig. 6. Hence, with increasing adsorbent mass, the amount of phenol adsorbed onto unit

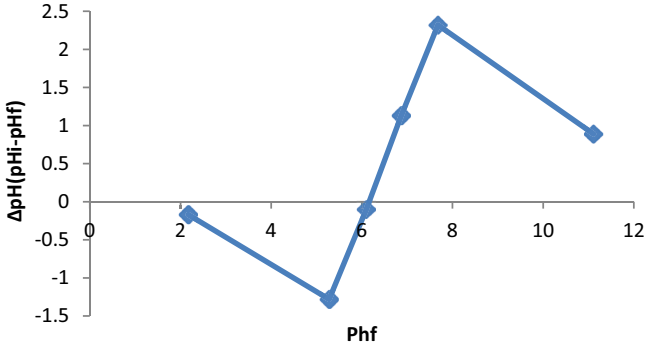

Fig. 2. Determining the point of zero charge.

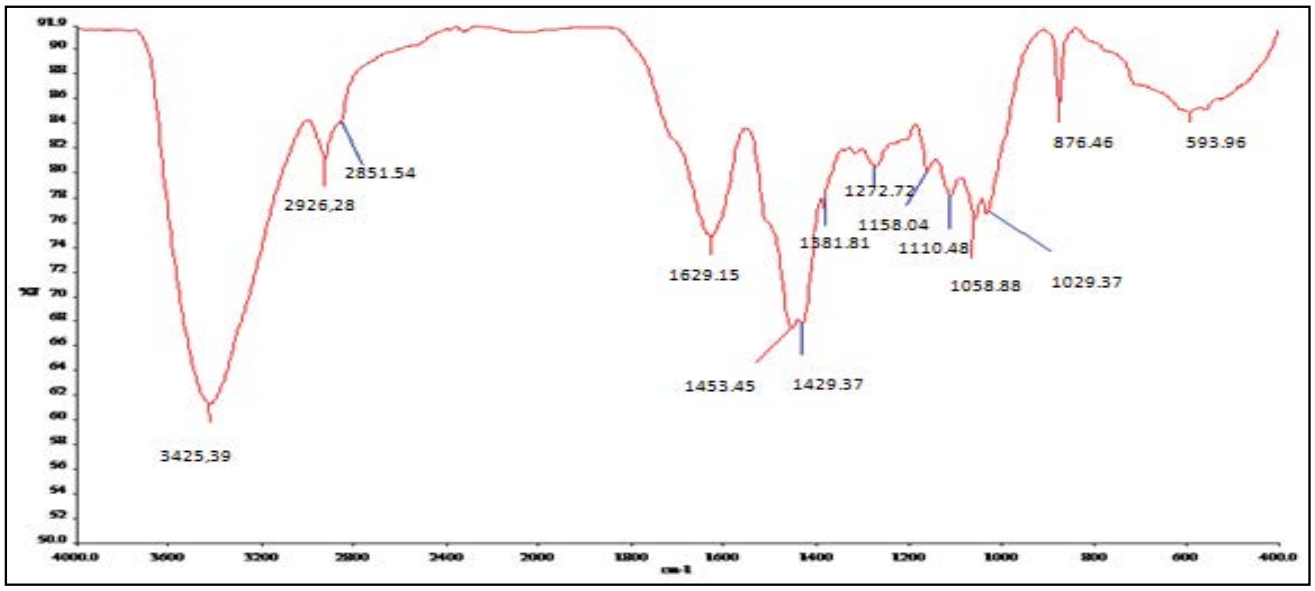

Fig. 3. FTIR spectra of PAPC.

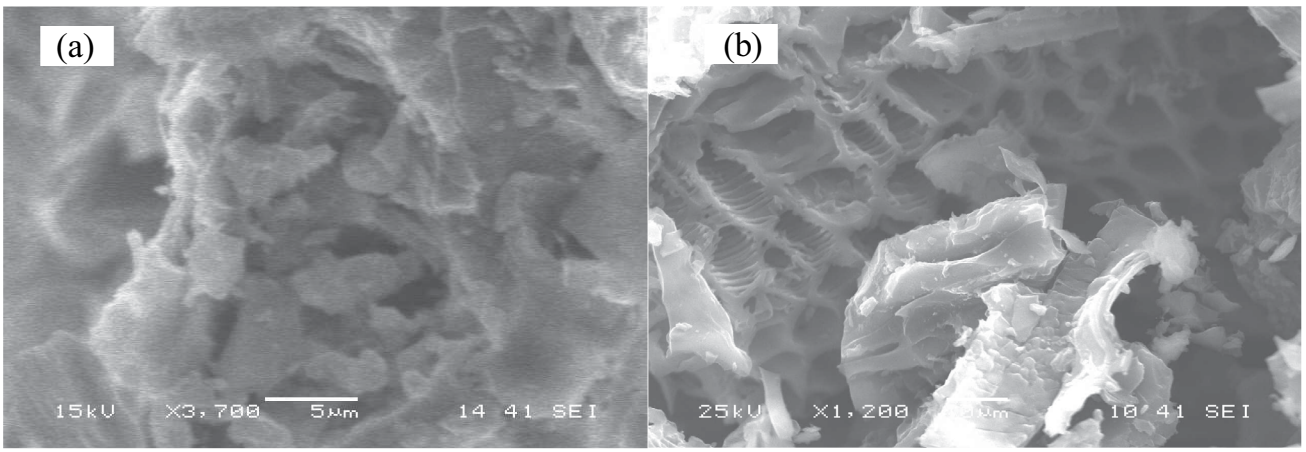

Fig. 4. SEM photographs of powdered raw pine cone (a) and powder activated pine cone PAPC (b).

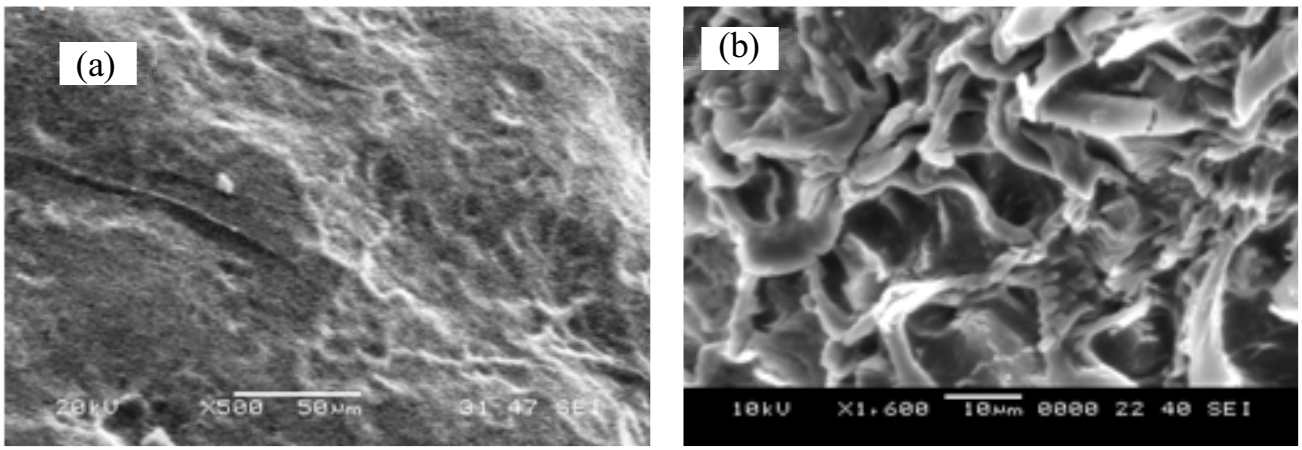

Fig. 5. SEM photographs of alginate beads (a) and alginate-PAPC beads (b).

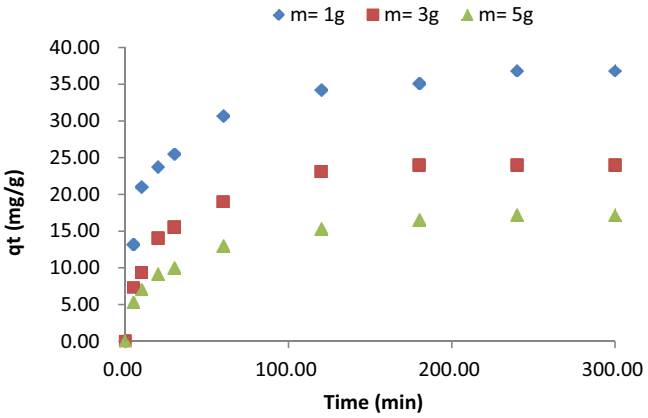

Fig. 6. Effect of adsorbent mass on the adsorption capacity of phenol by alginate-PAPC beads.

weight of adsorbent gets reduced, causing a decrease in the adsorption capacity with the increasing of the adsorbent mass concentration.

3.4. Effect of the initial concentration

Fig. 7 illustrates the effect of the initial phenol concentration on the adsorption capacity by alginate-PAPC beads in the range of phenol concentrations 20–500 mg/L and a ratio of 1 g of alginate beads/500 mL volume solution. It can be seen that for each initial concentration, the adsorption capacity of phenol increased gradually with the increasing contact time and reached its optimum level. Also, an increase in initial phenol concentration leads to an increase in the adsorption capacity of phenol onto PAPC-Alginate beads. This can be explained by the increase in the mass transfer driving force as the initial phenol concentration increased. Higher initial phenol concentration provides a stronger driving force of the concentration gradient resulting in higher adsorption capacity [40]. At a lower initial phenol concentration, there will be unoccupied active sites on the adsorbent surface.

3.5. Effect of pH medium

Fig. 8 shows that when the initial pH increases, the adsorption capacity of phenol decreased. A maximum

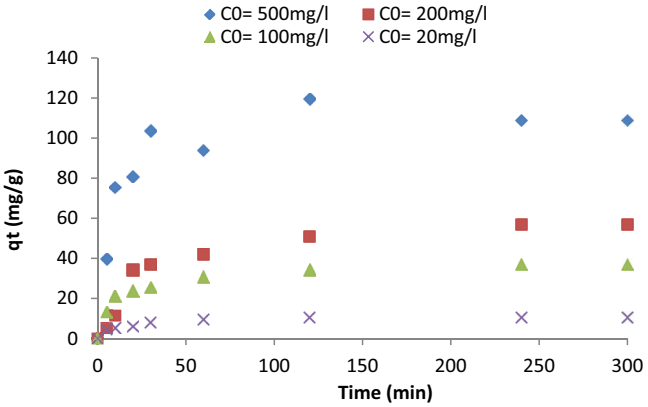

Fig. 7. Effect of initial concentration of phenol on the adsorption capacity by alginate-PAPC beads.

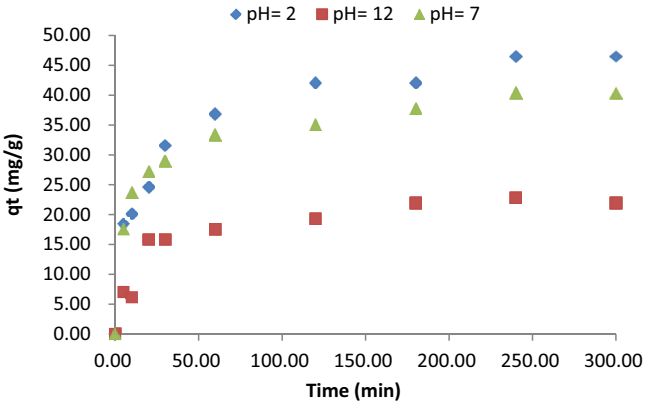

Fig. 8. Effect of pH on the adsorption capacity of phenol by alginate-PAPC beads.

adsorption capacity of 46.49 mg/g is observed at the optimum pH of 2. It appears that in the acid state, the positive charge is dominant on the surface of the adsorbent. This means that a substantially high electrostatic attraction exists between the positive charges of the adsorbent surface and the negative charges of the phenolates formed, which favors the adsorption [41]. On the other hand, in the alkaline environment, the dominant charge of the adsorbent surface is negative; this decreases the adsorption due to the repulsive force between the phenolate ion and the negative charge of the carbon surface of the phenolates bearing the same charge [17].

3.6. Equilibrium isotherms

The adsorption isotherms indicate how the sorbate is distributed between the liquid and the solid phases when the sorption process reaches an equilibrium state and provide information on the capacity of the adsorbent. Three widely used models, Langmuir, Freundlich, and Temkin were applied for the fitting of the experimental data [41]. The Langmuir equation shown below seems suitable for a monolayer sorption onto a homogeneous surface with the negligible interaction between adsorbed molecules.

$$\frac{C_e}{q_e} = \frac{1}{q_{\max} K_l} + \frac{1}{q_{\max}} C_e \tag{3}$$

The Freundlich isotherm model assumes heterogeneous adsorptive energies on the adsorbent surface and can be written as:

$$\log q_e = \log k_f + \frac{1}{n} \log C_e \tag{4}$$

where C_e is the equilibrium concentration of phenol (mg/L) in the solution, q_e is the amount of phenol adsorbed per unit mass of adsorbent (mg/g). K_L is the Langmuir equilibrium constant (L/mg), and $q_{\max}$ (mg/g) is the maximum adsorption capacity.

The essential characteristics of Langmuir isotherm can be expressed by a dimensionless constant R_L, which is defined by the following equation:

$$R_L = \frac{1}{1 + K_L C_0} \tag{5}$$

The value of R_L indicates the shape of the isotherm to be either unfavorable ($R_L > 1$), linear ($R_L = 1$), favorable ($0 < R_L < 1$), or irreversible ($R_L = 0$).

K_F and "n" are Freundlich constants related to the adsorption capacity and adsorption intensity, respectively.

The Temkin isotherm assumes that the heat of adsorption (function of temperature) of all molecules in the layer would decrease linearly rather than logarithmic with coverage. The model is expressed in the following equation:

$$q_e = B \ln K_T + B \ln C_e \tag{6}$$

The Temkin constant "B" is related to the heat of adsorption (kJ/mol). K_T is the equilibrium binding constant (L/mol) corresponding to the maximum binding energy.

The fitted parameter values are listed in Table 1, and the model curves are plotted in Fig. 9.

As seen from Table 1, the experimental data were well described by both Langmuir (R^2 = 0.992) and Freundlich (R^2 = 0.977) isotherms, with a possibility of mono and heterolayer phenol formation on the adsorbent surface. Temkin isotherm also showed a good fit with R^2 = 0.964.

For the Freundlich isotherm, the plot of log q_e versus log C_e gives a straight line with a slope of $1/n$ as shown in Fig. 9. The value of $1/n$ of 0.499 indicates a favorable adsorption of phenol on alginate-PAPC beads.

Moreover, the Temkin isotherm was studied to explore the Gibbs free energy change as:

$$B = \frac{RT}{\Delta G°} \tag{7}$$

R is the gas constant (8.314 J/mol.°K), and T is the absolute temperature (°K).

Table 1
Langmuir, Freundlich, and Temkin isotherm model parameters for adsorption of phenol on alginate-PACP beads.

Models	Freundlich			Langmuir			Temkin		
Parameters	K_F (L/g)	$1/n$	R^2	q_{max} (mg/g)	K_L (L/mg)	R^2	K_T (L/g)	B	R^2
Values	4.4375	0.499	0.977	66.666	0.027	0.992	0.393	12.405	0.964

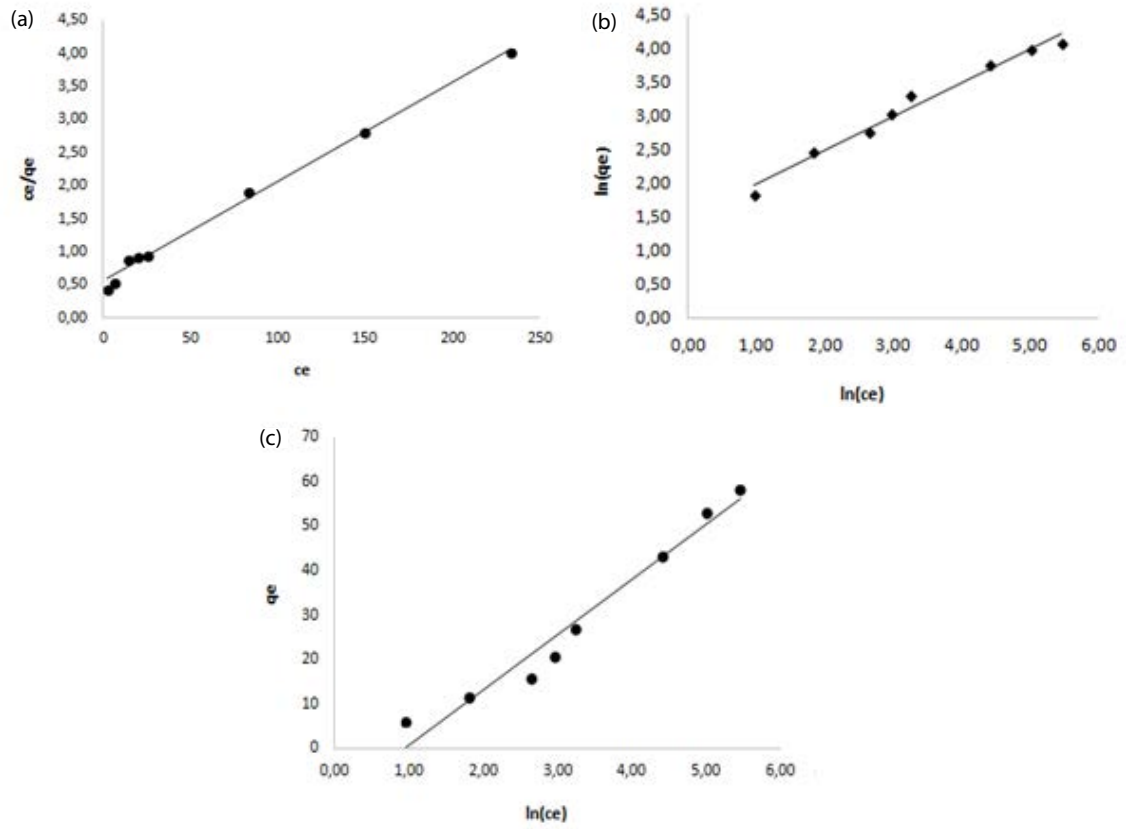

Fig. 9. Adsorption isotherms of phenol on alginate-PAPC beads: (a) Langmuir, (b) Freundlich, and (c) Temkin.

The value of DG° is 0,199 KJ/mol; that is, lower than 10 KJ/mol indicating a physical adsorption process.

Maximum monolayer adsorption capacity, q_{max} from the Langmuir model was 66.66 mg/g. The value of R_L was in the range of 0.648–0.069 indicating a favorable phenol adsorption on the alginate-PAPC beads.

By way of comparison, Table 2 indicates the adsorption of phenol on various alginate bioadsorbents from the literature.

3.7. Adsorption kinetic

Adsorption kinetic studies are important in the treatment of aqueous effluents because they provide valuable information on the mechanism of the adsorption process. In the present research, the kinetic data obtained from batch studies have been analyzed by pseudo-first-order and pseudo-second-order models and intraparticle diffusion model. The best fit model was selected based on the linear regression correlation coefficient R^2 values (Figs. 10–12).

The pseudo-first-order kinetic model frequently used in kinetic studies is generally expressed as follows:

$$\ln\left(q_e - q_t\right) = \ln q_t - k_1 t \tag{8}$$

where q_e and q_t are the amounts of phenol adsorbed (mg/g) at equilibrium and at time t (min), respectively, and k_1 is the rate constant of pseudo-first-order sorption (mg/g.min).

The pseudo-second-order kinetic model frequently used in kinetic studies is generally expressed as follows:

$$\frac{t}{q_t} = \frac{1}{k_2 q_e^2} + \frac{1}{q_e} t \tag{9}$$

where k_2 (g/mg.min) is the equilibrium rate constant for the pseudo-second-order adsorption and can be obtained from the plot of t/q_t against t.

In the case of the intraparticle diffusion model, the adsorption proceeds in several steps involving transport solute molecules from the aqueous phase to the surface of the solid particles and then the interior of the solid. According to Weber and Morris [44], for most adsorption processes the amount of adsorption varies almost proportional with $t^{1/2}$, which can be expressed:

$$q_t = k_i t^{1/2} + C \tag{10}$$

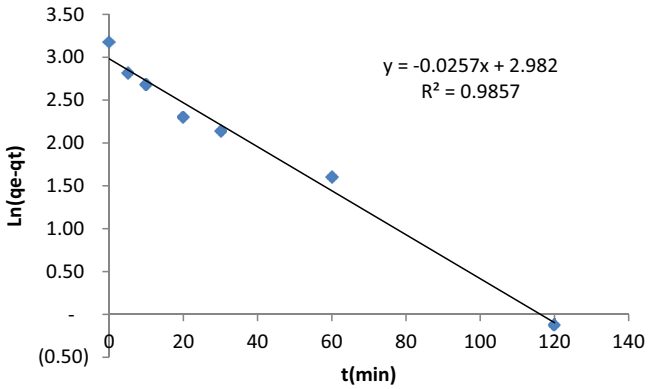

Fig. 10. Pseudo-first-order model.

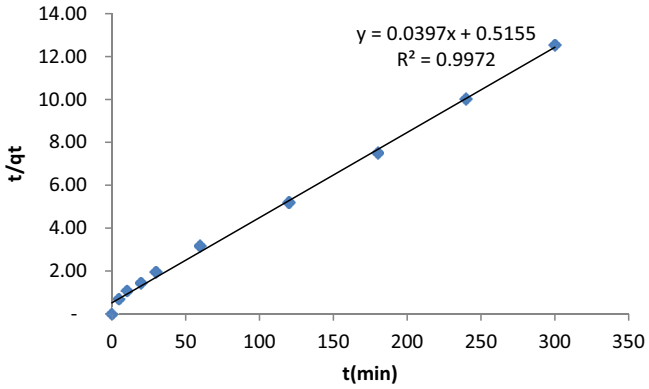

Fig. 11. Pseudo-second-order model.

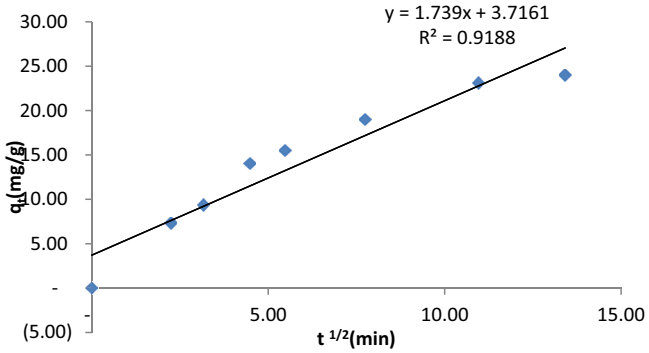

Fig. 12. Intraparticle diffusion model.

Table 2
Comparison of maximum phenol adsorption capacity obtained in this study with previous data

Adsorbents	Maximum adsorption capacities (mg/g)	References
Alginate-PAC beads	146.39	This study
Phenyltrimethylammonium-bentonite alginate beads	142	[27]
Octadecyltrimethylammonium-bentonite alginate beads	392	[27]
Hexadecyltrimethylammonium-bentonite alginate beads	185	[27]
Alginate–bentonite beads	235.761	[42]
Chitosan–calcium alginate blended beads	108.7	[43]

q_t is the amount of sorbate adsorbed at time t; C (mg/g) is the intercept and k_i is the intraparticle diffusion rate constant (mg/g.min$^{1/2}$).

All kinetic data for the adsorption of phenol onto alginate activated carbon beads, calculated from the related plots, are summarized in Table 3. The validity of the exploited models is verified by the correlation coefficient, R^2. Comparison of the R^2 values for different models suggests that the pseudo-second-order kinetic model fits best because of its highest value ($R^2 = 0.997$). Pseudo-second-order kinetic model implies that the predominant process here is chemisorption, which involves a sharing of electrons between the adsorbate and the surface of the adsorbent. Chemisorption is usually restricted to just one layer of molecules on the surface, although it may be followed by additional layers of physically adsorbed molecules [45].

3.8. Factorial design analysis

In this study, a full 2^3 factorial design was used for modeling the adsorption process. Three factors were considered: initial phenol concentration (X_1), pH (X_2), and adsorbent dose (X_3). The levels and ranges of these factors are given in Table 4.

The response "Y" values indicate the experimental adsorption capacity at equilibrium time (q_e). The results of experimental design (Table 5) were studied and interpreted by JMP8 to estimate the response values.

The coded mathematical model used for 2^3 factorial designs can be given as:

$$Y = a_0 + a_1X_1 + a_2X_2 + a_3X_3 + a_{12}X_1X_2 + a_{23}X_2X_3 + a_{123}X_1X_2X_3 \quad (11)$$

where Y is the estimated response, a_0 is the global mean; a_i and a_{ij} represent the regression coefficient corresponding to the main factor effects and interactions, respectively.

The estimates of the coefficients of Eq. (11) are given in Table 5, as well as the values of the standard error, t-value and Prob. > $|t|$. The mathematical model of the factorial design is then given as follows:

$$Y = 47.778 + 40.7175X_1 - 11.185X_2 - 15.0575X_3 - 7.8225X_1X_2 - 13.45X_1X_3 + 6.1425X_2X_3 + 4.24X_1X_2X_3 \quad (12)$$

Table 3
Kinetic model parameters for adsorption of phenol onto alginate-activated carbon beads

Kinetic model	First order		Second order		Intraparticle diffusion model	
Parameters	k_1 (mg/g.min)	R^2	k_2 (g/mg.min)	R^2	k_i (mg/g.min$^{1/2}$)	R^2
Values	0,025	0.985	0.0029	0.997	1.739	0.918

Table 4
Low and high levels of factors

Variables, unit	Factors	Levels		
		−1	0	+1
Initial phenol concentration (mg/L)	X_1	20	260	500
pH	X_2	2	7	12
PAPC mass (g/L)	X_3	1	2	3

Table 5
Full factorial design matrix of three variables in coded and natural units with the experimental responses

Run	Real values			Coded values			q_e (mg/g) observed value	q_e (mg/g) predicted value	Error
	C_0 (mg/L)	pH	PAPC mass (g)	X_1	X_2	X_3			
1	20	2	1	−1	−1	−1	12.28	13.933	−1.653
2	500	2	1	+1	−1	−1	144.74	146.393	−1.653
3	20	12	1	−1	+1	−1	1.75	3.403	−1.653
4	500	12	1	+1	+1	−1	85.96	87.613	−1.653
5	20	2	3	−1	−1	+1	5.26	6.913	−1.653
6	500	2	3	+1	−1	+1	66.96	68.613	−1.653
7	20	12	3	−1	+1	+1	2.34	3.993	−1.653
8	500	12	3	+1	+1	+1	49.71	51.363	−1.653
9	260	7	2	0	0	0	54.39	47.778	6.612
10	260	7	2	0	0	0	54.39	47.778	6.612

Fig. 13 shows the predicted values versus the experimental values of the equilibrium adsorption capacity. The high values for the coefficients of determination R^2 of R^2 adjusted (0.994 and 0.973) indicate a high level of significance for the model [42].

3.8.1. Student's t-test

The student's *t*-test was used to determine the significance of the regression coefficients of the parameters. A large *t*-value associated with a low *p*-value ($p < 0.05$) of a variable indicates a high significance of the corresponding model term [46].

Table 6 shows that the linear effects of the initial concentrations of phenol, adsorbent dose, pH medium, and the two interactions effects X_1X_2 and X_1X_3 are significant.

Considering that the interactions which have no statistical significance can be discarded, the final empirical model for the equilibrium capacity adsorption becomes:

$$Y = 47.778 + 40.7175X_1 - 11.185X_2 - 15.0575X_3 - 7.8225X_1X_2 - 13.45X_1X_3 \quad (13)$$

Based on the sign of each linear effect, the initial concentration of phenol has a positive effect on the equilibrium adsorption capacity.

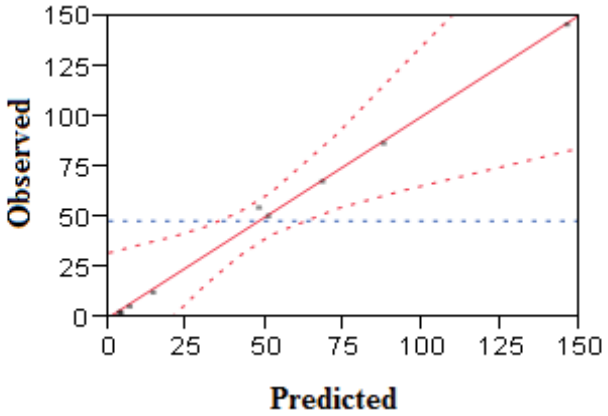

Fig. 13. Observed versus predicted equilibrium adsorption capacity.

Table 6
Estimated regression coefficients for the equilibrium adsorption capacity

Term	Estimate	Standard error	*T*-value	*p*-value
Constant	47.778	2.337695	20.44	0.0024
X_1	40.7175	2.613622	15.58	0.0041
X_2	−11.185	2.613622	−4.28	0.0505
X_3	−15.0575	2.613622	−5.76	0.0288
$X_1 \times X_2$	−7.8225	2.613622	−2.99	0.0959
$X_1 \times X_3$	−13.45	2.613622	−5.15	0.0357
$X_2 \times X_3$	6.1425	2.613622	2.35	0.1432
$X_1 \times X_2 \times X_3$	4.24	2.613622	1.62	0.2462

The pH medium and the mass of adsorbent have a negative effect on the equilibrium adsorption capacity

3.8.2. Interaction plots

The interactions plot presented in Fig. 14 shows the effect of each factor on the high and low levels of the second factor. Two of these interactions are significant and the most significant one with a negative value is between initial concentration of phenol and the mass of absorbent. This means that at low mass adsorbent, the equilibrium adsorption capacity increased when increasing the initial concentration of phenol.

The second significant interaction effect is between the initial phenol concentration and pH medium. Under an acid medium, the equilibrium adsorption capacity increased with increasing the initial phenol concentration.

3.8.3. Analysis of variance (ANOVA)

ANOVA results are shown in Table 7. The three sources of variation are model, error, and C. Total (corrected total sum of squares).

The *F* ratio (model mean square divided by the error mean square) tests the hypothesis that all the regression parameters (except the intercept) are zero. The null hypothesis is rejected if the *F* ratio is large

Prob. > *F* is the probability of obtaining a higher *F*-value by chance alone. Significance probabilities of 0.05 or less are often considered to indicate that there is at least one significant regression factor in the model [47].

As shown in Table 7, a very low probability (Prob. > *F*) = 0.0038 (<0.05), indicates that the models are statistically significant.

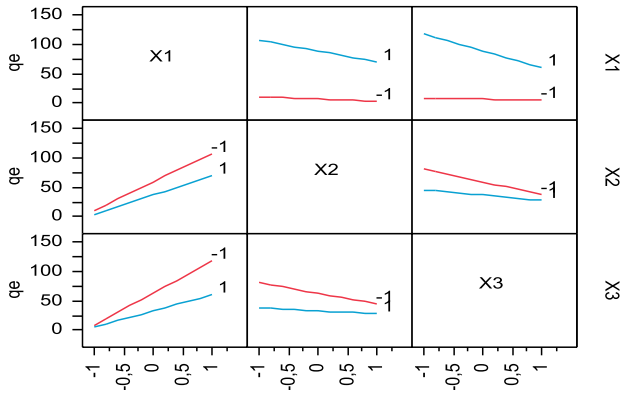

Fig. 14. Interaction plot for equilibrium adsorption capacity.

Table 7
Analysis of variance

Source	DF	Sum of square	Mean square	*F*-value	*p*-value
Model	5	18,014.731	3,602.95	25.9691	0.0038*
Residual	4	554.960	138.74		< 0.05
C. Total	9	18,569.69	/		

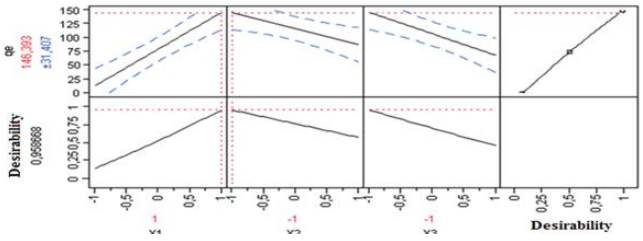

Fig. 15. Desirability functions for optimization of the response.

3.8.4. Optimization by desirability function

The desirability approach function was used to obtain the optimum conditions corresponding to maximum equilibrium adsorption capacity.

A desirability scale value of one means the optimum property level of the response whereas zero desirability indicates an unacceptable response.

As shown in Fig. 15, the highest equilibrium adsorption capacity of phenol was theoretically predicted to be 146.39 mg/g, at which the initial phenol concentration was 500 mg/L, adsorbent dose 1g/L, and pH medium 2.

4. Conclusions

In this study, powdered activated pine cone in alginate beads was used for the elimination of phenol from aqueous solutions. The equilibrium data were well fitted by Langmuir, Freundlich, and Temkin models. To evaluate the effect of initial phenol concentration, pH medium, and mass of adsorbent on the equilibrium adsorption capacity, a full factorial design approach was carried out. The results indicated that the three parameters are significant at the experimental range studied. The value of R^2 and R^2 adjust > 0.90 for the present mathematical model indicates a high correlation between observed and predicted values.

The higher equilibrium adsorption capacity was about 146.39 mg/g and corresponds to the following conditions: initial phenol concentration 500 mg/L, pH medium 2, and mass of PAPC 1 g.

References

[1] A. Ali, K. Saeed, Phenol removal from aqueous medium using chemically modified banana peels as low-cost adsorbent, Desal. Wat. Treat., 57 (2016) 11242–11254.
[2] W. Lazli, D. Hank, S. Zeboudj, A. Namane, A. Hellal, Application of factorial experimental design methodology for the removal of phenol from water by innovate hybrid bioprocess, Desal. Wat. Treat., 57 (2015) 1–7.
[3] T. Senthilvelan, J. Kanagaraj, R.C. Panda, A.B. Mandal, Biodegradation of phenol by mixed microbial culture: an eco-friendly approach for the pollution reduction, Clean Technol. Environ. Policy, 16 (2013) 113–126.
[4] V. Vaiano, M. Matarangolo, J.J. Murcia, H. Rojas, J.A. Navío, M.C. Hidalgo, Enhanced photocatalytic removal of phenol from aqueous solutions using ZnO modified with Ag, Appl. Catal. B: Environ., 225 (2018) 197–206.
[5] M.L.A. Fernández, M. Espino, F.J.V. Gomez, M.F. Silva, Novel approaches mediated by tailor-made green solvents for the extraction of phenolic compounds from agro-food industrial by-products, Food Chem., 239 (2018) 671–678.
[6] H. Hassan, B. Jin, E. Donner, S. Vasileiadis, C. Saint, S. Dai, Microbial community and bioelectrochemical activities in MFC for degrading phenol and producing electricity: Microbial consortia could make differences, Chem. Eng. J., 332 (2018) 647–657.
[7] M. Carmona, A.D. Lucas, J.L. Valverde, B. Velasco, J.F. Rodríguez, Combined adsorption and ion exchange equilibrium of phenol on Amberlite IRA-420, Chem. Eng. J., 117 (2006) 155–160.
[8] B.D. Reinoso, A. Moure, J. González, H. Domínguez, A membrane process for the recovery of a concentrated phenolic product from white vinasses, Chem. Eng. J., 327 (2017) 210–217.
[9] X. Zhang, Q. Li, J. Wang, J. Li, C. Zhao, D. Hou, Effects of feed solution pH and draw solution concentration on the performance of phenolic compounds removal in forward osmosis process, J. Environ. Chem. Eng., 5 (2017) 2508–2514.
[10] Y. Li, X. Hu, X. Liu, Y. Zhang, Q. Zhao, P.N.S. Tian, Adsorption behavior of phenol by reversible surfactant-modified montmorillonite: mechanism, thermodynamics, and regeneration, Chem. Eng. J., 334 (2018) 1214–1221.
[11] J. Han, Z. Du, W. Zou, H. Li, C. Zhang, In-situ improved phenol adsorption at ions-enrichment interface of porous adsorbent for simultaneous removal of copper ions and phenol, Chem. Eng. J., 262 (2015) 571–578.
[12] X. Gao, Y. Dai, Y. Zhang, F. Fu, Effective adsorption of phenolic compound from aqueous solutions on activated semi coke, J. Phys. Chem. Solids, 102 (2017) 142–150.
[13] L. Lupa, L. Cocheci, R. Pode, I. Hulka, Phenol adsorption using Aliquat 336 functionalized Zn-Al layered double hydroxide, Sep. Purif. Technol., 196 (2018) 82–95.
[14] D. Zhang, P. Huo, W. Liu, Behavior of phenol adsorption on thermal modified activated carbon, Chin. J. Chem. Eng., 24 (2016) 446–452.
[15] M.H. Al-Malack, M. Dauda, Competitive adsorption of cadmium and phenol on activated carbon produced from municipal sludge, J. Environ. Chem. Eng., 5 (2017) 2718–2729.
[16] L. Giraldo, J.C.M. Piraján, Study of adsorption of phenol on activated carbons obtained from eggshells, J. Anal. App. Pyrol., 106 (2014) 41–47.
[17] U. Beker, B. Ganbold, H. Dertli, D.D. Gülbayir, Adsorption of phenol by activated carbon: influence of activation methods and solution pH, Energy Convers. Manage., 51 (2010) 235–240.
[18] D.L. Postai, C.A. Demarchi, F. Zanatta, D.C.C. Melo, C.A. Rodrigues, Adsorption of rhodamine B and methylene blue dyes using waste of seeds of *Aleurites moluccana*, a low cost adsorbent, Alex. Eng. J., 55 (2016) 1713–1723.
[19] O.A. Oyewo, M.S. Onyango, C. Wolkersdorfer, Application of banana peels nanosorbent for the removal of radioactive minerals from real mine water, J. Environ. Radioact., 164 (2016) 369–376.
[20] D. Sana, S. Jalila, A comparative study of adsorption and regeneration with different agricultural wastes as adsorbents for the removal of methylene blue from aqueous solution, Chinese. J. Chem. Eng., 25 (2017) 1282–1287.
[21] A. Saxena, M. Bhardwaj, T. Allen, S. Kumar, R. Sahney, Adsorption of heavy metals from wastewater using agricultural–industrial wastes as biosorbents Open access, Wat. Sci., 31 (2017) 189–197.
[22] Y. Chen, F. Wang, L. Duan, H. Yang, J. Gao, Tetracycline adsorption onto rice husk ash, an agricultural waste: Its kinetic and thermodynamic studies, J. Mol. Liq., 222 (2016) 487–494.
[23] M. Kalaruban, P. Loganathan, W.G. Shim, J. Kandasamy, S. Vigneswaran, Enhanced removal of nitrate from water using amine-grafted agricultural wastes, Sci. Total Environ., 565 (2016) 503–510.
[24] A. Kumar, H.M. Jena, Removal of methylene blue and phenol onto prepared activated carbon from Fox nutshell by chemical activation in batch and fixed-bed column, J. Clean. Prod., 137 (2016) 1246–1259.
[25] R.S. Ingole, D.H. Lataye, P.T. Dhorabe, Adsorption of phenol onto Banana Peels Activated Carbon, KSCE. J. Civ. Eng., 21 (2017) 100–110.
[26] B. Biswas, N. Pandey, Y. Bisht, R. Singh, J. Kumar, T. Bhaskar, Pyrolysis of agricultural biomass residues: comparative study of corn cob, wheat straw, rice straw and rice husk, Biores. Technol., 237 (2017) 57–63.

[27] G. Derafa, H. Zaghouane-Boudiaf, C.V. Ibbora, Preparation and characterization of new low cost adsorbent beads based on activated bentonite encapsulated with calcium alginate for removal of 2,4-dichlorophenol from aqueous medium, Int. J. Biol. Macromol., 115 (2018) 257–265.
[28] S.K. Behera, H. Meena, S. Chakraborty, B.C. Meikap, Application of response surface methodology (RSM) for optimization of leaching parameters for ash reduction from low-grad coal, Int. J. Min. Sci. Technol., 28 (2018) 621–629.
[29] R.H. Myers, D.C. Montgomery, Response Surface 1 Methodology – Process and Product Optimization Using Designed Experiments, 2nd ed., John Wiley & Sons, New York, 2002.
[30] J. Goupy, L. Creighton, Introduction aux plans d'expériences, Third ed., Dunod, France, 2006.
[31] T.Y. Kim, H.J. Jin, S.S. Park, S.J. Kim, S.Y. Cho, Adsorption equilibrium of copper ion and phenol by powdered activated carbon, alginate bead and alginate-activated carbon bead, J. Ind. Eng. Chem., 14 (2008) 714–719.
[32] B. Agarwal, C. Balomajumder, P.K. Thakur, Simultaneous co-adsorptive removal of phenol and cyanide from binary solution using granular activated carbon, J. Chem. Eng., 228 (2013) 655–664.
[33] A.E. Ofomaja, E.B. Naidoo, S.J. Modise, Removal of copper (II) from aqueous solution by pine and base modified pine cone powder as biosorbent, J. Hazard. Mater., 168 (2009) 909–917.
[34] T.K. Sen, S. Afroze, H. Ang, Equilibrium, kinetics and mechanism of removal of methylene blue from aqueous solution by adsorption onto pine cone biomass of *Pinus radiate*, Wat. Air Soil Pollut., 218 (2011) 499–515.
[35] S. Dawood, T.K. Sen, Removal of anionic dye Congo red from aqueous solution by raw pine and acid-treated pine cone powder as adsorbent: equilibrium, thermodynamic, kinetics, mechanism and process design, Water Res., 46 (2012) 1933–46.
[36] A.E. Ofomaja, E.B. Naidoo, Biosorption of copper from aqueous solution by chemically activated pine cone: a kinetic study, J. Chem. Eng., 175 (2011) 260–270.
[37] M. Momcilovic, M. Purenovic, A. Bojic, A. Zarubica, M. Randelovic, Removal of lead(II) ions from aqueous solutions by adsorption onto pine cone activated carbon, Desalination, 276 (2011) 53–59.
[38] N.M. Mahmoodi, B. Hayati, M. Arami, C. Lan, Adsorption of textile dyes on Pine Cone from colored wastewater: kinetic, equilibrium and thermodynamic studies, Desalination, 268 (2011) 117–125.
[39] M.T. Yagub, T.K. Sen, H. Ang, Equilibrium, kinetics, and thermodynamics of methylene blue adsorption by pine tree leaves, Wat. Air Soil Pollut., 223 (2012) 5267–5282.
[40] M.A. Ahmad, N.A. Ahmad Puad, O.S. Bello, Kinetic, equilibrium and thermodynamic studies of synthetic dye removal using pomegranate peel activated carbon prepared by microwave-induced KOH activation, Water Resour. Ind., 6 (2014) 18–35.
[41] A. Khaled, A.E. Nemr, A. El-Sikaily, O. Abdelwahab, Removal of Direct N Blue-106 from artificial textile dye effluent using activated carbon from orange peel: adsorption isotherm and kinetic studies, J. Hazard. Mater., 165 (2009) 100–110.
[42] D. Hank, Z. Azi, S. Ait Hocine, O. Chaalal, A. Hellal, Optimization of phenol adsorption onto bentonite by factorial design methodology, J. Ind. Eng. Chem., 20 (2014) 2256–2263.
[43] S.K. Nadavala, K. Swayampakula, V.M. Boddu, K. Abburi, Biosorption of phenol and o-chlorophenol from aqueous solutions onto chitosan–calcium alginate blended beads, J. Hazard. Mater., 162 (2009) 482–489.
[44] W.J. Weber, J.C. Morris, Kinetics of adsorption on carbon from solutions, J. Sanit. Eng. Div., 89 (1963) 31–60.
[45] E.N. El Qada, S.J. Allen, G.M. Walker, Adsorption of Methylene Blue onto activated carbon produced from steam activated bituminous coal: a study of equilibrium adsorption isotherm, Chem. Eng. J., 124 (2006) 103–110.
[46] H. Harfouchi, D. Hank, A. Hellal, Response surface methodology for the elimination of humic substances from water by coagulation using powdered Saddled sea bream scale as coagulant-aid, Process Saf. Environ. Protect., 99 (2016) 216–226.
[47] O. Freitas, C. Delerue-Matosb, R. Boaventura, Optimization of Cu (II) biosorption onto *Ascophyllum nodosum* by factorial design methodology, J. Hazard Mater., 167 (2009) 449–454.